

We are IntechOpen, the world's leading publisher of Open Access books Built by scientists, for scientists

6,900

Open access books available

186,000

International authors and editors

200M

Downloads

Our authors are among the

154

Countries delivered to

TOP 1%

most cited scientists

12.2%

Contributors from top 500 universities



WEB OF SCIENCE™

Selection of our books indexed in the Book Citation Index
in Web of Science™ Core Collection (BKCI)

Interested in publishing with us?
Contact book.department@intechopen.com

Numbers displayed above are based on latest data collected.
For more information visit www.intechopen.com



Near-Field Antenna of RFID System

Zijian Xing

Additional information is available at the end of the chapter

<http://dx.doi.org/10.5772/intechopen.71427>

Abstract

Radio frequency identification (RFID) technology is a very important part of the Internet of Things. The antenna used in RFID system reader is one of its most important equipment, has become a research hotspot. Compared to far-field applications, RFID antennas typically use high-gain circularly polarized antennas or antenna arrays to increase their read distance. Near-field RFID reader antenna requires strong magnetic field, wide band and low gain characteristics, while the resulting magnetic field should be evenly distributed to avoid leakage read phenomenon. The main contents of this chapter are as follows. The RFID reader near field antenna based on the principle of magnetic field coupling has developed rapidly in recent years. In this paper, a double-layer open-circuit antenna are proposed. The near-field antennas have wideband and strong magnetic field characteristics, and are compact and simple to process. The open-loop antenna of the double-layer terminal is located at the lower level and the upper layer is the radiation ring. The antenna size is smaller, and the feeder part and the radiation part of the isolation, a good deal to avoid interference between each other.

Keywords: RFID, near field, antenna, electrically large

1. Concept of near-field antenna

Radio frequency identification (RFID) technologies, which were developed during the World War II, provide wireless identification and tracking capability [1, 2]. The reader antenna is an important unit of RFID systems. Many new RFID antennas are developed for different applications [3–7]. Reader antennas can be classified into two types based on the working scope for different application purposes: near-field antenna and far-field antenna. Currently, ultra-high frequency (UHF) near-field RFID technology are fast developed in item-level identifications such as sensitive products tracking, biological products and medical products (blood, medicines, vaccines), biosensing applications and so on [8–12].

The basic consideration of UHF near-field RFID is to make it work in a short distance stable, just like what LF/HF near-field RFID does [8]. Inductive coupling systems are selected in most applications in near-field UHF RFID, because most of the reactive energy is stored in magnetic field. Inductive coupling is more stable than the capacitive coupling and hardly affected by liquid or metal [13].

In a near-field RFID system, the reader and the tag antennas are coupled mainly through magnetic field. If the tag antenna is electrically small, the magnetic field of reader antenna is perturbed by tag rarely, and coupling coefficient C could be shown by the equation [14, 15].

$$C \propto f^2 N_{\text{tag}}^2 S_{\text{tag}}^2 B^2 \alpha \quad (1)$$

where f is an operating frequency, N_{tag} is the number of turns of the tag coil, S is the cross-section area of the coil, B is the magnetic field density at the tag location and α is the antenna misalignment loss.

One of the challenges in UHF near-field RFID applications is to design a reader antenna with wide bandwidth and strong near magnetic field simultaneously. Strong near magnetic field is important for extending the reading range. Low gain could reduce interferences. Wide bandwidth antenna could be applied at 840–960 MHz, which covers both ETSI of Europe and FCC of North America. In some special application scenarios, smaller size antennas are required because of the limited system space.

Some near-field antennas have been reported to generate strong and even magnetic field. Many travelling wave antenna is proposed to extend the bandwidth [16]. A conventional travelling wave antenna called Mini-Guardrail from a famous company Impinj has wide bandwidth of more than 200 MHz at UHF band as well as low gain [17]. But because, loads of traveling wave antenna consume too much power, current and near magnetic field are not strong enough. The magnetic field should be lower than -13 dBA/m at any direction if the distance above antenna is larger than 2 cm. Conventional standing wave antenna could present a strong magnetic field, but its gain is too high and bandwidth is too narrow to cover a wide UHF RFID bandwidth. Typical standing wave antenna with strong magnetic field like eye shape is proposed by Li et al. [18], but -10 dB bandwidth is only 30 MHz which could only cover FCC band. Narrow bandwidth antenna is easily detuned by environmental changes.

2. Typical design of electrically large near-field RFID antenna

2.1. Structure and character of a near-field RFID antenna

The current distribution of the near-field antenna is in-phase. That is, the current on the loops has the same orientation. For example, a two-layer and open circuit shape near-field antenna made by PCB board is shown in **Figure 1**. The current character is explained by this example.

Figure 1(a) shows the structure of the antenna, which is composed of two PCB layers. The top layer is mainly composed of two quasi-half loops which are connected with two folded

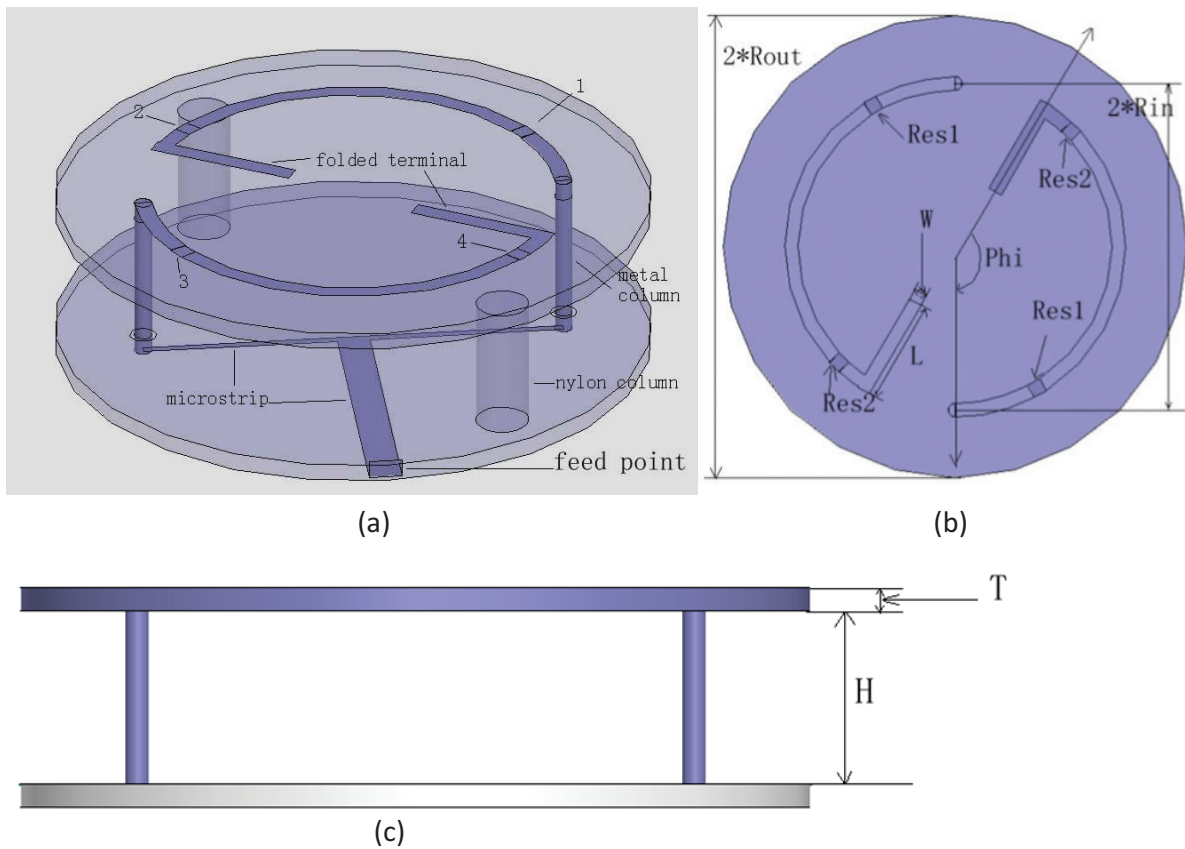


Figure 1. Model and structure of the proposed antenna: (a) 3D view, (b) top view and (c) side view.

straight terminals. The bottom layer is feed network with ground and lead are printed onto top and bottom surface, respectively. Fed at edge of bottom layer, 50 ohm microstrip line is connected with two 100-ohm lines, which are connected to two metal columns in another end. The other end of each column is connected to metal quasi-half loop strip. There are four loads on two quasi-half loops which are marked by 1, 2, 3 and 4 in **Figure 1(a)**. The two PCB boards are connected by two metal columns and fixed by two nylon columns.

Figure 1(b) shows the top view. Angle and radius of loop are marked by Φ and R_{in} , respectively. Length of folded terminal, width of metal strip and radius of PCB board are marked by L , W and R_{out} , respectively. The value of loads 1, 3 is $Res1$ and 2, 4 is $Res2$. **Figure 1(c)** shows the side view. The distance between two PCB layers and thickness of top PCB board are marked by H and T , respectively. Bottom layer has the same size and material as top layer.

2.2. Performance of the antenna

The proposed antenna can be printed onto any substrate and optimized at specific operating frequency by properly selecting the geometrical parameters. The antenna prototype is printed onto a FR4 substrate ($\epsilon_r = 4.4$, $\tan\delta = 0.02$, thickness $T = 2$ mm). The optimized antenna has parameters of $H = 15$ mm, $W = 2$ mm, $R_{in} = 25$ mm, $R_{out} = 34$ mm, $Res1 = 30$ ohm, $Res2 = 50$ ohm, $L = 8$ mm and $T = 2$ mm. As shown in **Figure 2(a)** and **(b)**, the antenna is fed by SMA port on the edge of the bottom layer. The new proposed antenna has many advantages such as strong magnetic field, low far-field gain, wide bandwidth, small size and so on.

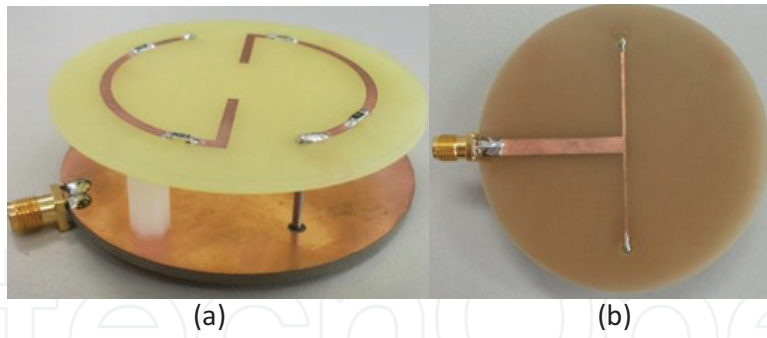


Figure 2. Photograph of the antenna: (a) 45° view of the antenna and (b) bottom view of the antenna.

2.2.1. S11 performance

The impedance matching measurement of the antennas was carried out using the Agilent N5230A vector network analyzer. Figure 3 shows the simulated and measured return loss. The proposed antenna exhibits broadband impedance bandwidth, the frequency range for -15 dB return loss is from 826 to 950 MHz or 124 MHz bandwidth. The measured result agrees well with the simulation.

2.2.2. Far-field gain and directivity

The far-field gain and directivity are shown in Figure 4. It is clear that the gain is lower than -10 dB at any direction and about 15 dB lower than directivity.

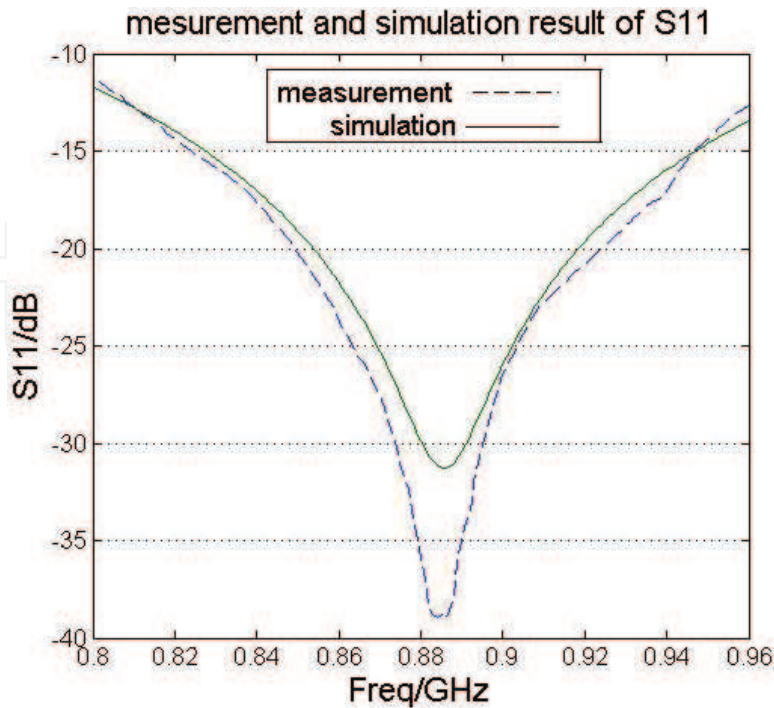


Figure 3. S11 of the actual antenna and simulation model.

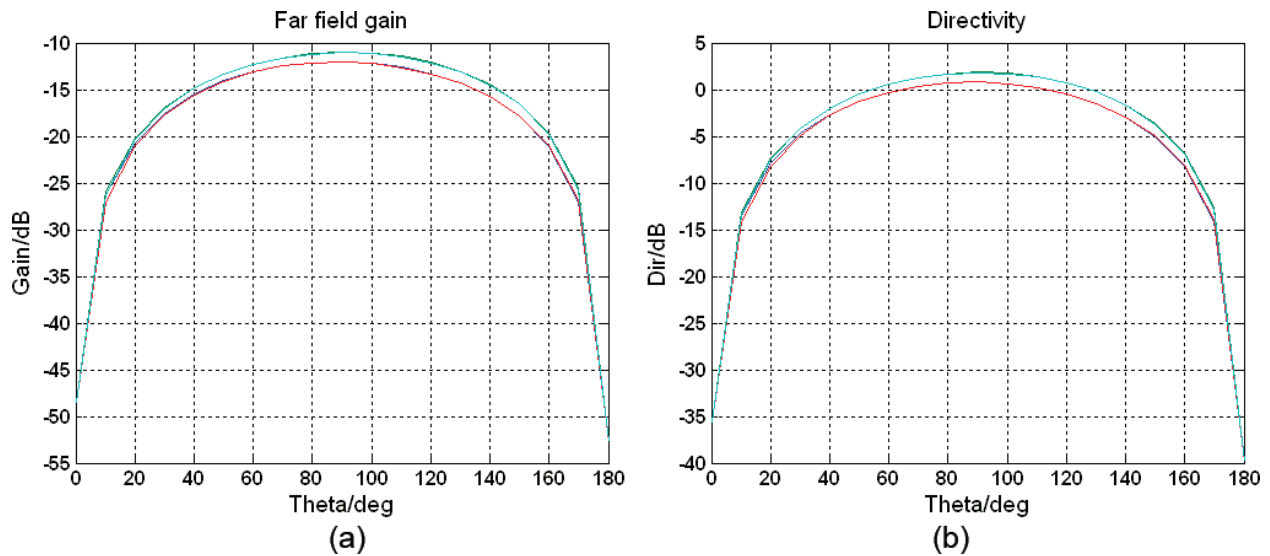


Figure 4. (a) Far-field gain versus theta at different Φ , which is 0, 90, 180 and 270°, and marked by four curves; (b) directivity versus theta at different Φ which is same as (a).

2.2.3. Current distribution

Figure 5 shows the current distribution of different phases. Different from conventional traveling wave antenna, current on the loop assumes standing wave distribution. One important factor of current is in-phase. Because magnetic field produced by the currents on the adjacent sides of the antenna cancel out each other and is thus very weak in the central portion of interrogation zone if the current distribution is out-phase. In **Figure 5**, current of this antenna is not out-phase because of small electrical length of the quasi-half loop. At the phases of 45, 90 and 135 degree, the currents are all strong. Actually, the magnetic field at these phases are also strong. The result could be verified by the comparison between **Figures 5** and **6**.

2.2.4. Magnetic field distribution

Figure 6 shows that magnetic field is concentrated and uniform around the center region of antenna at different phases (0°, 45°, 90°, 135°). Moreover, as a result of folded terminal, average current can be enhanced on the outer loop so that strong magnetic field intensity is obtained.

Figure 7(a) shows the magnetic field distribution at different z above the surface of antenna's top. The reason for choosing such a graduation scale is narrowly related with reading tag ability which will be discussed later. **Figure 7(b)** focuses on the magnetic field intensity attenuation versus z -axis.

Compared to other antenna, it could be found that the z -orientation magnetic field of the new antenna is much stronger. For example, referred by **Figure 7(b)**, the magnetic field of this antenna is significantly stronger than that of the proposed traveling wave antenna in [17] at same z . At $z = 2$ cm, two-layer and two quasi-half loops antenna has magnetic field intensity of -3 dBA/m, whereas the antenna from [17] has only -15 dBA/m. Taken **Figure 7(a)** as a reference, the magnetic field in center region of the antenna is also stronger than the another broadband

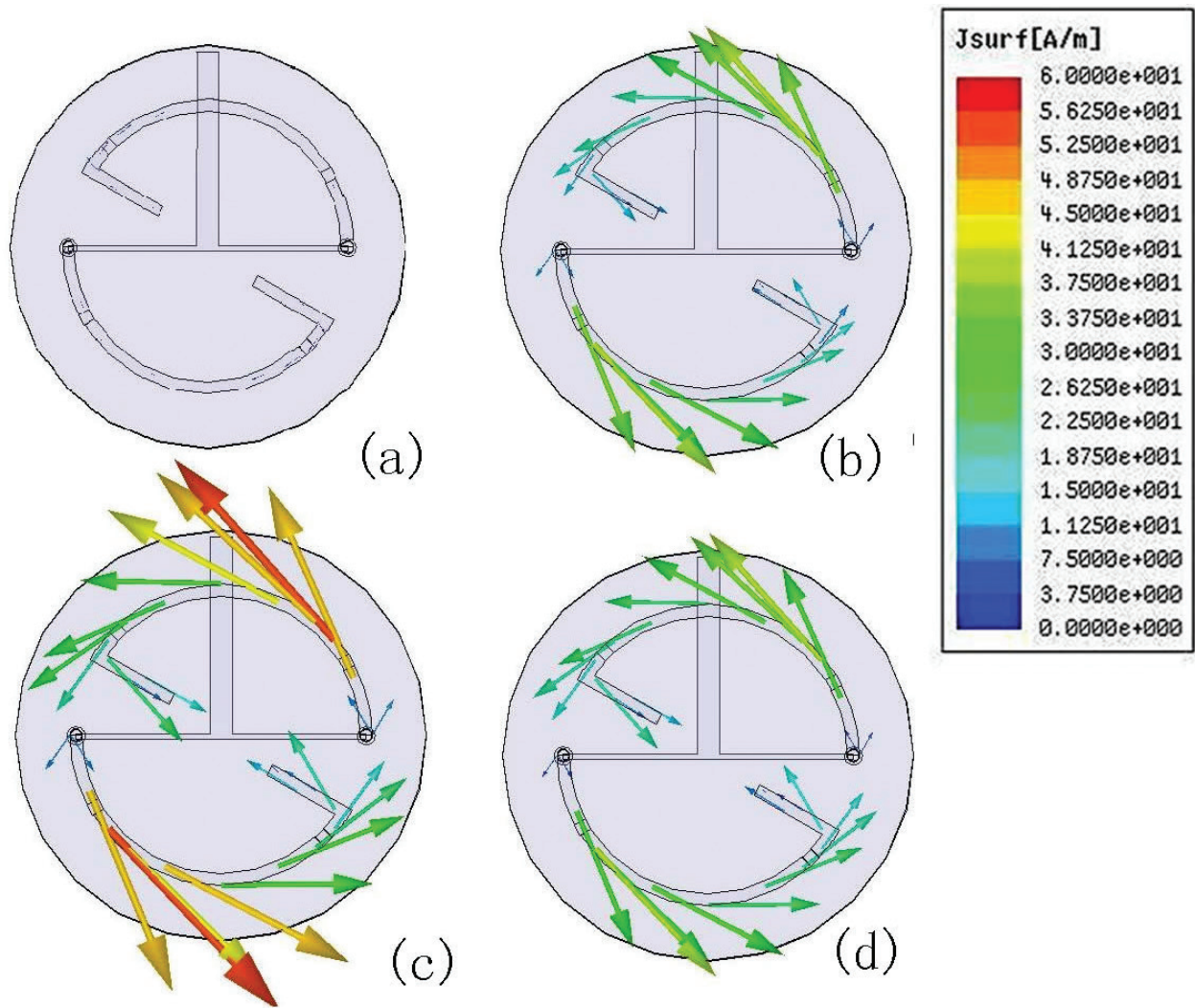


Figure 5. Current distribution on metal strip at different phases: (a) 0°, (b) 45°, (c) 90° and (d) 135°.

antenna which is proposed by Qing et al. [19]. It shows that magnetic field of the antenna from [19] is lower than -10 dBA/m at $z = 0.5$ mm, whereas two-layer and two quasi-half loops antenna is stronger than 0 dBA/m although at $z = 1$ cm.

2.3. Reading range

To further verify the performance of the proposed two-layer and two quasi-half loops antenna, the prototype was used as the reader antenna in a UHF near-field RFID system to detect UHF near-field tags. Test system is shown in **Figure 8(a)**, and the proposed antenna was connected to the reader operating at both 865–868 MHz of ETSI and 902–928 MHz of FCC with 30 dBm output to detect tag. Tag is positioned on a foam board, which has a size of 70 mm×70 mm, could be shown as **Figure 8(b)**. Grid is marked on the top of the foam board with the size of 1 cm×1 cm. The data of detected tag on each intersection were recorded.

This chapter adopts one annular tag which could be activated when magnetic field intensity is stronger than -13 dBA/m. The system choose ETSI band as the operating frequency because the operating mechanism of FCC is hopping frequency (HF).

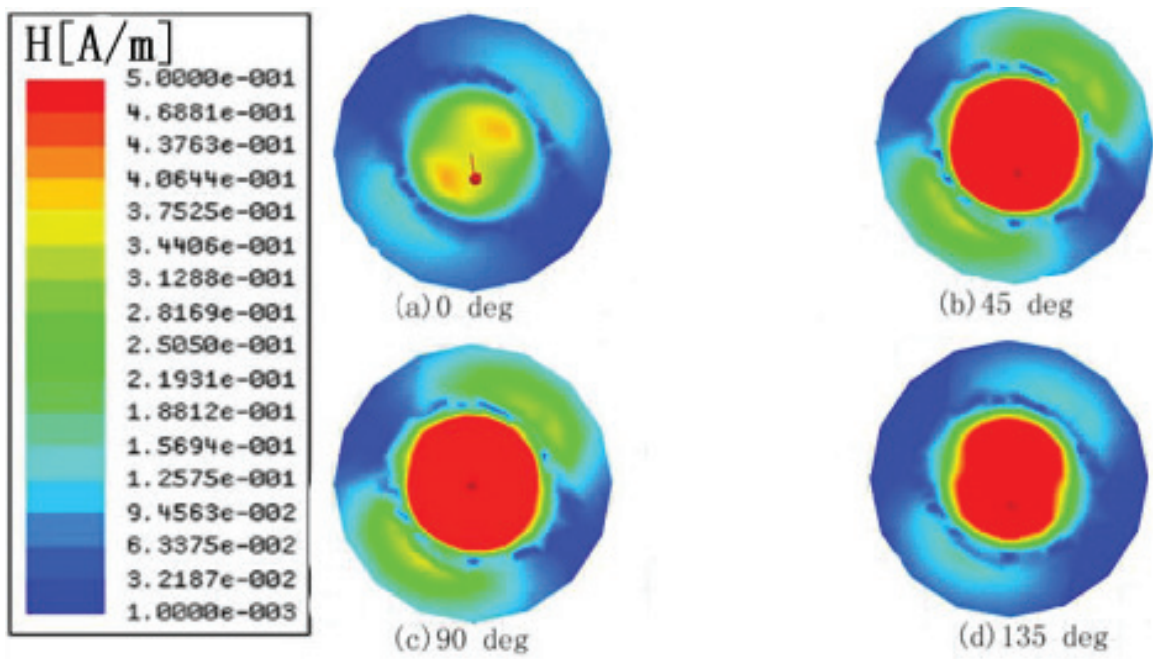


Figure 6. Different phases of z-orientation magnetic field distribution on the reference plane which is 1 cm above the top of antenna: (a) 0°; (b) 45°; (c) 90° and (d) 135°.

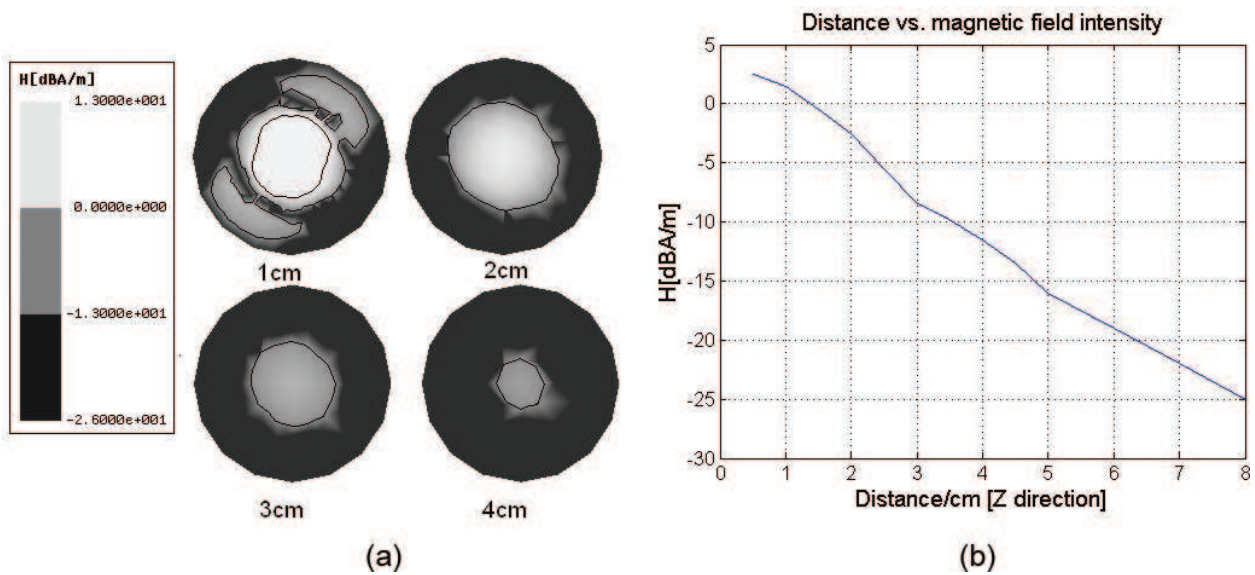


Figure 7. Simulated magnetic field distribution of the antenna operated at 868 MHz: (a) z-orientation magnetic field distribution at different z . Radius of reference plane is also 50 mm and (b) magnetic field intensity of the antennas along z -axis.

The measurement results of reading range are exhibited in **Figure 9**; it is clear that reading scope is reduced if distance increased. Compared between **Figures 9** and **7(a)**, it could be found that at each z , the reading range has a rough agreement with the magnetic field level line of -13 $dB(A/m)$. This is the reason for choosing such a graduation scale of z-orientation magnetic field in **Figure 7(a)**.

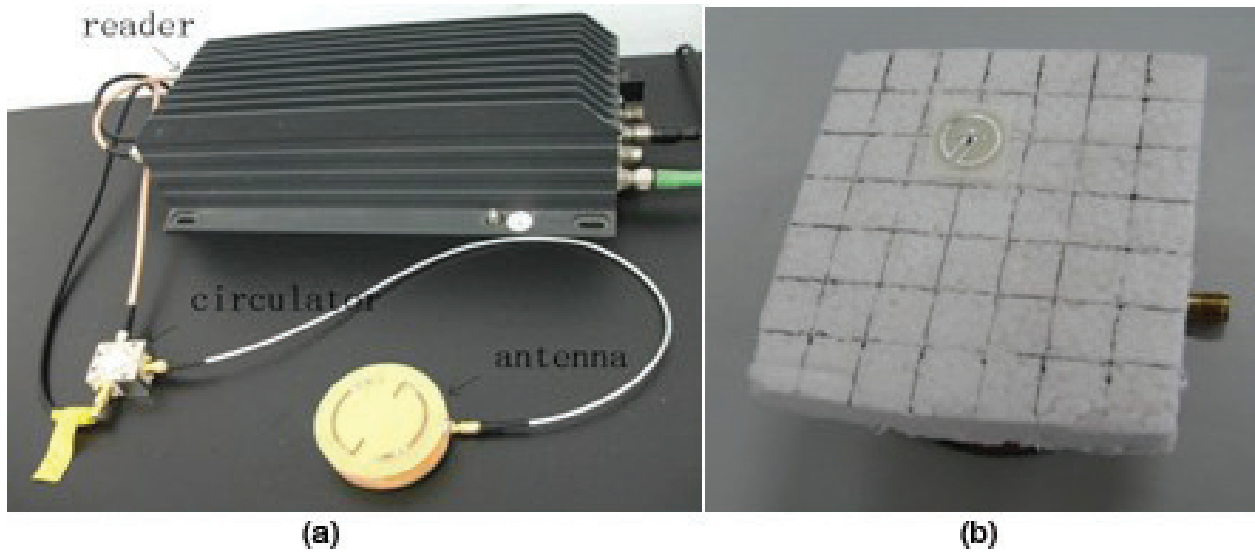


Figure 8. The configuration of reading range measurement. (a) Configuration of measurement scenarios: reader antenna, circulator and reader, which are connected with computer. (b) Foam board with tag is positioned above the antenna.

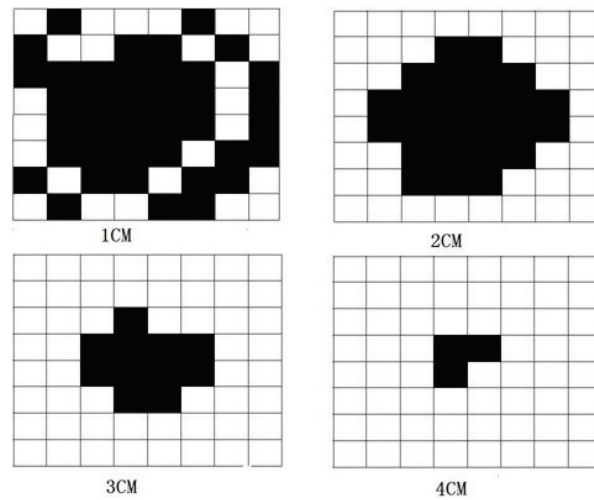


Figure 9. Reading scope of antenna at different distances, which are 1, 2, 3 and 4 cm. Black grid marked the intersection which could be read when tag is put on it, and white grid marked the opposite.

3. Optimization of near magnetic field

3.1. Parameter studies

The antenna's structure is a distorted symmetrical dipole. So, the length of metal loops and the input impedance could be estimated based on dipole theory. If resonant frequency is determined, the electric length of a metal column, quasi-half loop and folded terminal should match the resonant frequency.

$$L_{\text{loop}} = \frac{\text{phi}}{180} * \pi * R_{in} \quad (2)$$

where L_{loop} is the length of one quasi-half loop. It is needed to consider the quasi-half loop's mirror image function on the ground plane of microstrip during designing. Metal columns should be long enough because current mirror image is reversal and then it will cancel out a part of magnetic field. But if metal column is too long, magnetic field will be weak for the weak current on small quasi-half loop because of the unchangeable resonant frequency. Phase and magnitude of the current on both quasi-half loops are symmetrical so that magnetic field can be strengthened simultaneously by two quasi-half loops. Most of energy consumption of the antenna attributes to ohmic consumption on metal and loads, which could sharply reduce gain and broaden the bandwidth.

After extensive simulations, it is found that loads ($Res1$ and $Res2$), the length of H and L_{loop} affect antenna performance significantly, whereas the other parameters show slight effects. The antenna with the parameters: $R_{out}=34$ mm, $R_{in}=25$ mm, $\Phi=160$ degree, $L=8$ mm, $W=2$ mm, $Res1=30$ ohm, $Res2=50$ ohm, $H=15$ mm and $T=2$ mm was selected as a reference. All the simulation results of magnetic field distribution in this chapter are z -orientation. In this section, magnetic field is observed on the reference plane = 1 cm above the top of the antenna with radius of 50 mm. Set the upper surface of top layer as $z=0$, so that the distance between reference plane and antenna could be figured by the value of z . z -axis passes through the center of both top and bottom PCB boards.

3.1.1. Loads on quasi-half loops, $Res1$ and $Res2$

Figure 10(a) and **(b)** shows the magnetic field distribution of antennas at different values of $Res1$ and $Res2$, respectively. It is observed that magnetic field distribution is sharply reduced with the increasing of $Res1$ and $Res2$ at the operating frequency. As shown in **Tables 1** and **2**, it could be found that the bandwidth and magnitude of S_{11} are also narrowly related with $Res1$ and $Res2$.

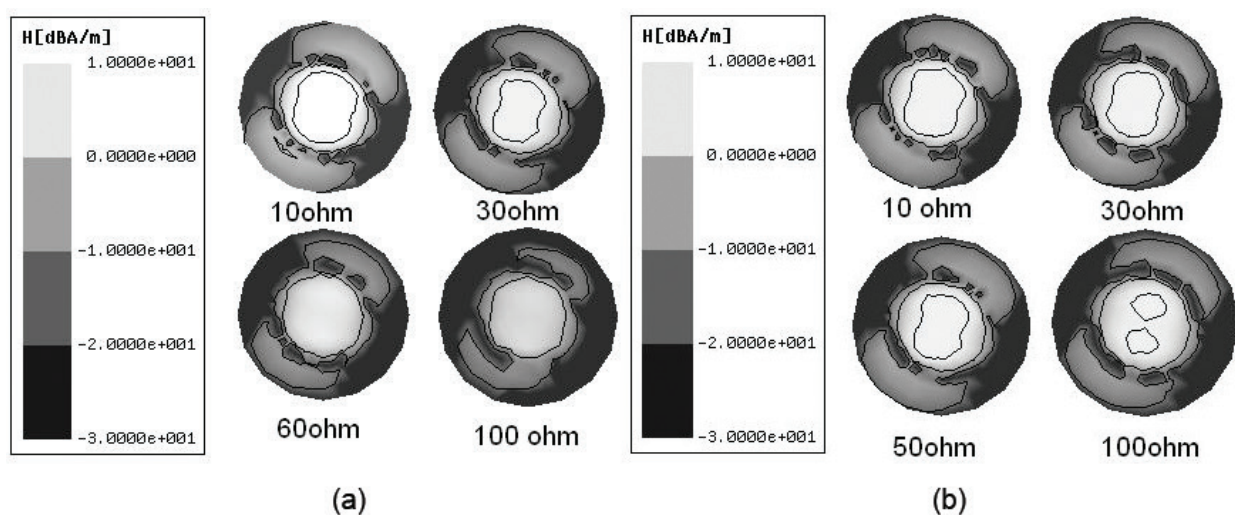


Figure 10. The relationship between loads and magnetic field at 868 MHz: (a) $Res1$ versus magnetic field and (b) $Res2$ versus magnetic field.

| <i>Res1</i> | S11 at resonant frequency | -15 dB bandwidth | -10 dB bandwidth |
|-------------|---------------------------|-----------------------|-----------------------|
| 10 ohm | -11.95 dB at 884 MHz | 0 MHz | 61 MHz (859–920 MHz) |
| 30 ohm | -33.5 dB at 884 MHz | 123 MHz (828–951 MHz) | 190 MHz (808–998 MHz) |
| 60 ohm | -13.81 dB at 884 MHz | 0 MHz | 179 MHz (818–986 MHz) |
| 100 ohm | -8.35 dB at 893 MHz | 0 MHz | 0 MHz |

Table 1. Relationship between the *Res1*, resonant frequency and bandwidth.

| <i>Res2</i> | S11 at resonant frequency | -15 dB bandwidth | -10 dB bandwidth |
|-------------|---------------------------|-----------------------|-----------------------|
| 10 ohm | -16.7 dB at 877 MHz | 42 MHz (857–899 MHz) | 124 MHz (817–941 MHz) |
| 30 ohm | -21.7 dB at 879 MHz | 72 MHz (844–916 MHz) | 145 MHz (810–955 MHz) |
| 50 ohm | -33.5 dB at 884 MHz | 123 MHz (828–951 MHz) | 190 MHz (808–998 MHz) |
| 90 ohm | -25.4 dB at 894 MHz | 96 MHz (850–946 MHz) | 184 MHz (811–996 MHz) |

Table 2. Relationship between the *Res2*, resonant frequency and bandwidth.

Both magnetic field and return loss are more sensitive to *Res1* than *Res2*, because the current of *Res1* is much stronger than that of *Res2*. From **Tables 1** and **2**, it is found that *Res1* or *Res2* affects resonant frequency slightly and bandwidth and S11 at resonant frequency significantly.

3.1.2. Effect of the space between two layers, *H*

Figure 11(a) and **(b)** exhibits the magnetic field distribution of the antennas with varying heights of *H* at 868 and 915 MHz. The antennas are configured with identical length of R_{in}

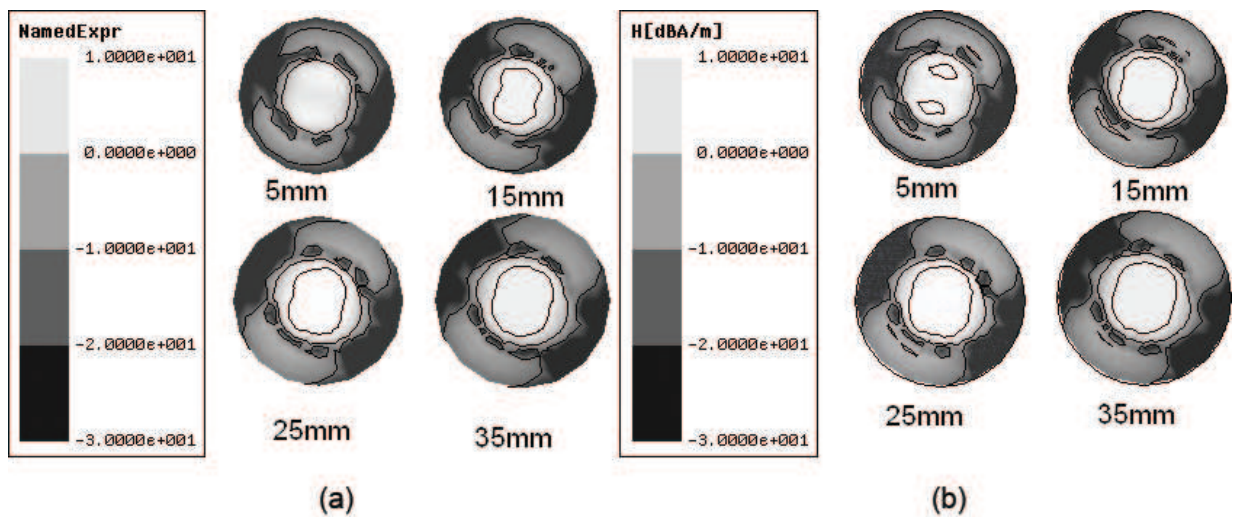


Figure 11. The relationship between the *H* and magnetic field at different frequencies: (a) 868 and (b) 915 MHz.

and L . It is observed that all the antennas have similar magnetic field except $H=5$ cm, when H changes from 5 to 35 mm. It could be inferred that the magnetic field is sharply cancelled out by current mirror image of the ground if H is too narrow. Current mirror image is too weak to influence the magnetic field when the length of H is longer than 15 mm.

3.1.3. Radius of quasi-half loop R_{in}

Radius of quasi-half loop is also an important influencing factor of magnetic field. In the experiments, other parameters are unchanged except R_{out} because radius of R_{out} is narrowly related with that of R_{in} . **Figure 12** shows how magnetic field changes with different R_{in} . It is clear that magnetic field should be weaker if the R_{in} is too small or large at 868 MHz. The total length of L_{loop} and L is far less than λ_4 (8.64 cm) and average current strength on the loop is naturally weak. But the reason for weak magnetic field at large R_{in} (40 mm) is the decentralization of magnetic field energy.

3.2. Structure improvement

Figure 13(a) shows the structure of the antenna. The top layer contains two quasi-half loops with two inductance-like terminals. The bottom layer is the feed network with the ground and lead. Fed at the edge, a 50 ohm microstrip line is connected to two 100 ohm microstrip lines which connect metal columns. The other end of each column is connected with a metal loop strip. On loops, there are four printed loads which are marked by 1, 2, 3 and 4 in **Figure 13(a)**. The two PCB boards are supported by two nylon columns.

Figure 13(b) shows the top view of antenna. The angle, width and radius of the quasi-half loop are marked by Φ , W and R_{in} , respectively. The radial and tangential length of the one circle of inductance structure is marked by L and BW , respectively. The number of the inductance loop is marked by N which is three in **Figure 13(b)**. Four resistors are printed on the top of antenna.

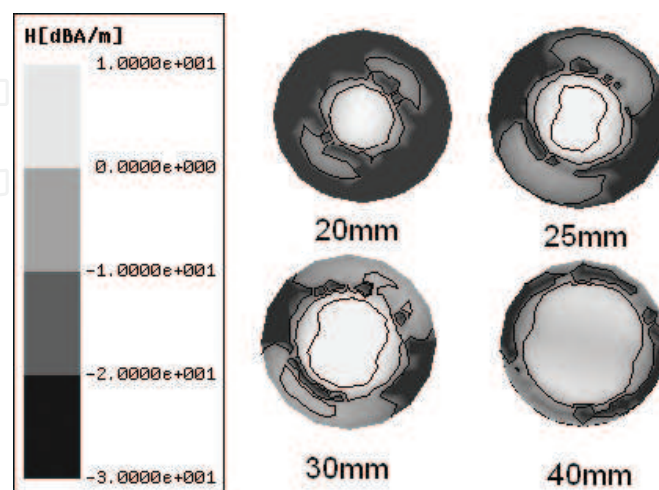


Figure 12. Magnetic field distribution of different R_{in} (868 MHz).

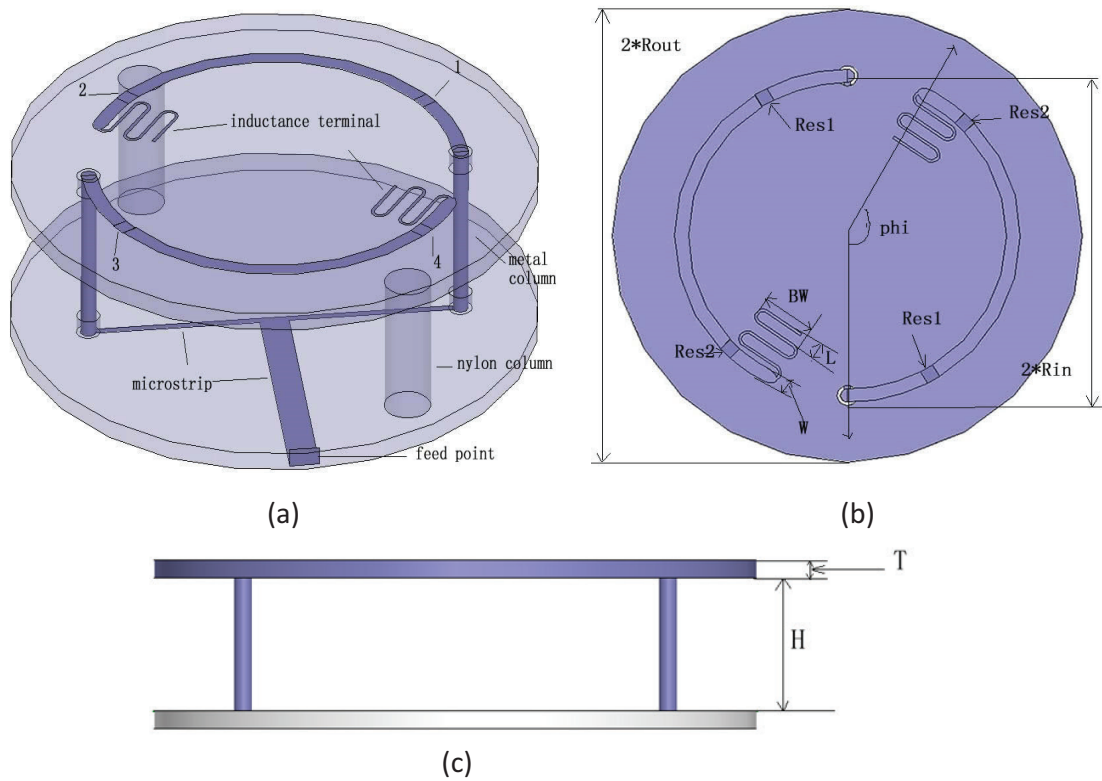


Figure 13. Model and structure of the proposed antenna: (a) 3D view, (b) top view and (c) side view.

4. Conclusion of near-field antenna of RFID system

It is challenging to design UHF near-field RFID antennas with strong magnetic fields and broad bandwidth. The UHF RFID antenna is demonstrated to be able to achieve a broad bandwidth and a low gain. The proposed antenna has also been proven to have strong magnetic fields with concentrated field distribution in the near-field region of antenna, which is very suitable for UHF near-field RFID reader applications.

Moreover, the investigation has shown that the UHF RFID antenna has produced the stronger magnetic field distribution. The most impact factor for near-field RFID antenna is magnetic field distribution. In recent years, near field radio frequency identification system has developed, many antennas are developed, but there are still have some problems. The combination of magnetic field construction and band widening technology is not perfect, especially the low-loss large-scale standing wave near-field antenna band widening technology is rarely reported.

The near-field theory is the research foundation of the near-field antenna. The breakthrough of the near-field electromagnetism theory and its innovation not only play an extremely important role in the development of the electromagnetism itself but also promotes the radio frequency identification directly and also a series of modern electronic technology development, so the analysis of the near-field problem is very basic in the electromagnetism, valuable and challenging research work.

Author details

Zijian Xing

Address all correspondence to: xingzijian2004@126.com

Northwestern Polytechnical University, China

References

- [1] Wantc R. An introduction to RFID technology. *IEEE Pervasive Computing*. 2006;**5**(1):25-33
- [2] Landt J. The history of RFID. *IEEE Potentials*. 2005;**24**(4):8-1
- [3] Cole PH. A Study of Factors Affecting the Design of EPC Antennas & Readers for Supermarket Shelves. Auto-ID Center, north terrace, adelaide, Australia; 2002
- [4] Liu ZM, Hillegass RR. A 3 patch near field antenna for conveyor bottom read in RFID sortation application. *Antennas and Propagation Society International Symposium 2006*, IEEE, July 2006, pp.1043-1046
- [5] Ranasinghe DC, Ng ML, Leong KS, Jamali B, Cole PH. Small UHF RFID label antenna Design and Limitations. 2006 IEEE International workshop on Antenna Technology, March 6-8, 2006, pp. 200-204
- [6] Nikitin PV, Rao KVS, Lazar S. An overview of near field UHF RFID, 2007 IEEE International Conference on RFID, Mar. 26-28, 2007, pp.166-174
- [7] Zhang M, Chen Y, Jiao Y, Zhang F. Dual circularly polarized antenna of compact structure for RFID application. *Journal of Electromagnetic Waves and Applications*. 2006;**20**(14):1895-1902
- [8] Harrop P. Near Field UHF vs. HF for Item Level Tagging [Online]. Available: http://www.eurotag.org/?Articles_and_Publications
- [9] Desmons D. UHF Gen2 for item-level tagging, presented at the RFID World 2006. [Online]. Available: www.impinj.com/files/Impinj_ILT_RFID_World.pdf
- [10] UHF Gen 2 for Item-Level Tagging Impinj RFID Technology Series Paper [Online]. Available: http://www.impinj.com/files/MR_GP_ED_00003_ILT.pdf
- [11] Ajluni C. Item-level RFID takes off. *RF Design Magazine*. Sep. 2006
- [12] Item-Level Visibility in the Pharmaceutical Supply Chain: A Comparison of HF and UHF RFID Technologies, Philips, TAGSYS, and Texas Instruments [Online]. Available: <http://www.tagsysrfid.com/modules/tagsys/upload/news/TAGSYSTI-Philips White-Paper.pdf>
- [13] Wang S, Guan X, Wang D-W, Ma X, Su Y. Fast Calculation of Wide-Band Responses of Complex Radar Targets. *Progress In Electromagnetics Research*. 2007;**68**:185-196

- [14] Qing X, Goh CK, Chen ZN. A broadband UHF near-field RFID antenna. *IEEE Transactions on Antennas and Propagation*. 2010;**58**(12)
- [15] Ryu H-K, Woo J-M. Size reduction in UHF band RFID tag antenna based on circular loop antenna. 18th International Conference on Applied Electromagnetics and Communications, 2005;12-14
- [16] Ling C. *Antenna Project Handbook*. Publishing House of Electronics Industry. Beijing, China; June 2002. p. 306-308
- [17] Mini Guardrail Antenna Datasheet [online]. Available: http://www.bodetech.com/documents/MiniGuardrail_Antenna_Datasheet.pdf
- [18] Li X, Liao J, Yuan Y, Yu D. Segmented coupling eye-shape UHF band near field antenna design. *IEEE Microwave Asia Pacific Conf*, Singapore, December 2009. pp. 2401-2404
- [19] Qing X, Chen ZN, Goh CK. UHF near field RFID reader antenna with capacitive couplers. *Electronics Letters*. 2010;**46**(24)